CrossMark

RESEARCH ARTICLE

Relationship Between Field-Based Plant Species Richness and Satellite-Derived Biophysical Proxies in the Western Ghats, India

Swapna Mahanand[1] · Mukunda Dev Behera[1,2]

Abstract Remote sensing offers fast and reliable technique to map the variation in plant diversity and distribution at different scales. Using 891 geo-tagged ground sampled point collected for the Western Ghats, India from a national level study on biodiversity characterization. We analyzed the distribution of plant species with respect to the satellite derived vegetation indices. The moderate resolution imaging spectroradiometer derived vegetation products, i.e., normalized difference vegetation index (NDVI), enhanced vegetation index (EVI), fraction of absorbed photosynthetically active radiation (fPAR), leaf area index (LAI), and surface reflectance (SR-645nm and SR-858nm) were fitted to suitable regression curves with respect to plant species richness where NDVI demonstrated the best fit ($R^2 = 0.07$); while fPAR showed ($R^2 = 0.08$) better relation with woody species richness. We observed positive but weak correlation for all the biophysiological proxies with species richness in the forests of Western Ghats. The annual pattern of correlation faired than seasonal (i.e., post-monsoon) between biophysical variables and species richness, while the woody subset of the species richness demonstrated marginally better relation at annual scale. The range of each biophysical proxy varied from medium to high, indicating higher vegetation strength. The species richness trend increased linearly for NDVI and EVI. The positive correlation showed by fPAR and LAI could be due to varied canopy architecture of the Western Ghats forests. Utility of fine resolution spatio-temporal data could render better understanding of species richness pattern using biophysical proxies, and thereby, help in long-term biodiversity monitoring.

Keywords MODIS · Reflectance · Species richness · Vegetation indices · Western Ghats

1 Introduction

Remote sensing is a technology which provides spatial information to map the plant productivity as stored potential energy that species reflect on the ground. The examination of the relationships between satellite derived biophysical proxies and biodiversity distribution is possible [1, 2]. With the free availability of coarse to high-resolution temporal satellite images, studies on productivity relationship with species richness have enhanced [3]. Remotely sensed estimates of biodiversity patterns are useful in decision making for land use and conservation. Usually, habitat heterogeneity allows more species to coexist that project higher spectral variations are expected to have the higher number of species [4]. It is expected that higher the spectral variability, higher the habitat and species variability [5]. Therefore, species richness and complementarity are convenient 'proxies' for plant diversity that can be estimated using spectral heterogeneity [6]. The spatial heterogeneity perceived by the remote sensors could be lower in forest ecosystems because of potentially similar canopy cover [7]. The variation in species number at the ground may alter the reflectance sensed by the remote sensor, similar to mirror-image relation [8]. Therefore, the satellite-derived information on vegetation can be used as a proxy for ground measured species richness.

✉ Swapna Mahanand
mahanand.swapna@gmail.com

1 School of Water Resources, IIT Kharagpur, Kharagpur, India

2 Centre for Oceans, Rivers, Atmosphere and Land Sciences, IIT Kharagpur, Kharagpur, India

🙋 Springer

Species richness (with 300 plots) regressed with Normalized difference vegetation index (NDVI) explained 76% of the variance in Hood river region of central Canadian arctic [9]. A study performed in Tuscany, Italy on a 380 ha nature reserve wetland using 22 plots (25 ha, plot size) was attempted to link field derived species richness with spectral properties from satellite data for investigating effects of mapping scales on the spatial and spectral resolution of images [10]. Mapping diversity patterns is accomplished by analyzing variation of some spectral signal, and correlating this variation with measures of species richness [11]. Furthermore, these researchers utilized 3954 plots for Kalahri woodland savannah and compared woody versus non-woody species richness for multi-sensor data. A better fitting of Moderate Resolution Imaging Spectroradiometer (MODIS) data was modeled for woody species compared with non-woody species [12].

Many researchers also use MODIS-derived enhanced vegetation index (EVI), Leaf Area Index (LAI), fraction of photosynthetically active radiation (fPAR), gross primary product (GPP) to measure species richness. The MODIS has two bands of surface reflectance: (1) red absorbance (620–670 nm or SR-645nm), and (2) infrared reflectance (841–876 nm or SR-858nm). The valid range of surface reflectance data is from 0 to 1. Basically, SR-645nm is the red absorbent region of the electromagnetic spectrum. Alternately, SR-858nm lies in the far-infrared region its properties are to reflect the vegetation from the ground. MODIS surface reflectance (MOD09A1) product was utilized along with its derived vegetation indices to analyze land surface phenology in the pixels containing the field plots for Qinling Mountains, China [13]. The ordination statistics inferred high temporal resolution land surface reflectance remote sensing data may be used as significant predictors of floristic ordination axes obtained using data from field surveys. For generalist species diversity and distribution measurement in a heterogeneous environment was improved when MODIS derived surface reflectance was integrated to habitat distribution mapping [14]. The cumulative effect of all spectral bands MODIS spatio-temporal data was mapped during winter and summer to identify the regulator variables of complex biosphere [15].

NDVI is sensitive to chlorophyll changes. It saturates at high biomass levels, and therefore not responsive to the full range of canopy. Rather, it saturates in dense forest canopy at intermediate values of LAI [16]. EVI is more sensible to variations in canopy structure, including LAI, canopy type, plant physiognomy, and canopy architecture. Usually, EVI fits better to address the change in canopy structure over a high biomass regions. The relationship between NDVI and species richness is reported to be positive. The correlation coefficient is weak depending on scales with variance <= 6% at 1 m^2 scale to 49% at 1 ha scale [17]. The

relationship between species richness and spectral reflectance observed to be poor ($R^2 = 0.1$) compared with the spectral derivatives [5]. The mixed pixels effects the relationships of spectral heterogeneity to species richness as observed weaker for LANDSAT-8 compared to the other two satellite images (RapidEye, ASTER) [18]. The tree species richness from low to high range was analyzed with NDVI and observed varied but good correlation ($R^2 = 0.66$) in a tropical forest [19]. Due to the presence of water in study site, i.e. Montepulciano Lake Reserve, Central Italy that severely affects the spectral response of the vegetation index, thus species richness and NDVI encountered with a weak correlation [10]. Using Landsat-derived normalized difference vegetation index (NDVI) the linkages between species richness–vegetation heterogeneity observed to be positive for Great Basin of western North America [20]. The MODIS GPP, NPP and NDVI were analyzed to explain species richness in North America [21]. MODIS derived standard deviation of GPP marked in grassland habitat, Normalized Difference Senescent Vegetation Index (maximum) in forests, and Land surface water index (average) in deserts are observed to be the best predictor of species richness in Semi-arid region of Inner Mongolia [22].

EVI is a refined version of NDVI, and its range varies between minimum -1 to maximum $+1$. The two vegetation indices are complementary to each other, the differences can be captured either during growing season or dense canopy [23]. EVI overall showed a better relationship and a lower root mean square error to measure greenness of vegetation than NDVI [24]. The response of MODIS derived NDVI and EVI tested towards the change in Amazon vegetation and observed 0.6 –0.8 units change in leaf area (2–6% change in NDVI) while no detectable change marked for EVI [25]. In a flood plain meadows, Loire River of Western Europe, to identify spatial surrogate for species richness tested with NDVI and EVI, where EVI ($R^2 = 0.61$) resulted best [26]. Also, the different derivatives of vegetation indices viz., standard deviation, annual maximum, seasonal maximum-minimum etc. observed to predict species richness better. With four different formulations of EVI (annual maximum, the annual integrated, and the growing season defined midpoint and growing season averaged values) the tree species diversity can explain up to 60% for 65 ecoregions in contiguous United States [27]. Leaf area index (LAI) and fraction of photosynthetically active radiation (0.4–0.7 mm) absorbed by vegetation (fPAR) are two key structural variables for vegetation [28]. MODIS derived LAI observed to be the most important variables parallel to other environmental variables derived from Quick Scatterometer, Shuttle Radar Topography Mission, and Tropical Rainfall Mapping Mission to predict tree species

richness and plant diversity [29].Using MODIS-LAI the distribution of woody needle leaf forest pattern fairly positive ($R^2 = 0.41$) as the influence of understory are limited in Ruokolahti coniferous forest, Finland [30]. The relationship between NDVI and woody species observed to be very high tested for urban forest area of Istanbul, Turkey [18].

The concept of using vegetation indices either derived from MODIS or other satellites to relate with species richness with different vegetation indices is rarely attempted [13, 14]. In India, the Western Ghats biodiversity was studied using satellite images to spatially identify the landscape elements [31]. Further, the relationship between NDVI and species richness evaluated using 59 plots laid in homogeneous strata and observed accuracy of 61% [32]. The linkage between species richness with spectral indices was attempted for Indian biogeographic region that suggested it's application on multilevel assesment of biodiversity [33]. In another study in the same region, species richness and normalized difference vegetation index (NDVI) were compared and found to be highly correlated [19]. A positive correlation was obtained between NDVI values and forest density in the western Himalaya region [34]. Higher resolution data showed a statistically significant correlation with species richness. An increasing number of studies cited the species–energy hypothesis while using NDVI to predict plant species richness [35]. But the large-scale spatial coverage by MODIS and providing vegetation indices at a high temporal scale is useful for large-scale early detection of ecological challenge.

Temporal environmental fluctuations such as seasonality define the ability of a habitat to support unique species at different times of the year that exert strong controls on biodiversity [36]. Through symbiotic interaction habitat sharing enhances recycling of nutrient in temporal variability [37]. The seasonal species germinated in post-monsoon with fresh pigments have high reflectance thus have more spectral variation in images, which get suppressed in annual scenario. Also, the growth of existing species get accelerate in the monsoon to post-monsoon period which derive the most floristic composition and pigments reflectance of a particular site. Hence, the variation in floristic composition vary with time and well addressed through seasonal variability. The annual variability summarized overall pattern of species distribution, mostly accounts the species have higher longevity that termed as perennial (woody species). This study attempts to correlate the field-based plant species richness with that of satellite-derived proxies of different diversity attributes. This is done by analyzing the species richness variation at (1) annual and post-monsoon period corresponding to capture the total and maximal plant growth; and (2) woody and non-woody categories in the Western Ghats region, India.

2 Methodology/Methodologies

2.1 Study Area

The shared biogeographical history introduced the Western Ghats of India and Sri Lanka listed as single unit and rank 21 among the 34 global biodiversity hotspot. Within a geographical area of 1, 25, 035 Km^2 bounded between 8°14′45″ to 21°52′40″ N latitude and 72°38′34″ to 78°26′18″ E longitude consists of 24 major vegetation types as per new vegetation types map of India [38]. The high levels of topographic and climatic heterogeneity supports the diverse vegetation types (abandoned jhum cultivation to tropical moist deciduous) and distinct fauna (amphibians-purple frog to mammals-*Panthera tigris*) in the Western Ghats [39]. Moving from north to south of study site, the positive correlation was observed between plant diversity and seasonality [40]. Similarly, the increase of plant endemism also reported in the direction of north to southern region [41]. It is also reported as the world's most densely populated biodiversity hotspot. Human invading to the hotspot that raising agricultural land, plantation, grazing and built-up brought the alteration in the composition of vegetation types, i.e., natural versus managed [42]. For this study, we simplified the new vegetation types for Western Ghats into forest and non-forest classes (Fig. 1a).

2.2 Flora Data

The diversity and distribution of species across India biogeographic zones were brought out through a study on Biodiversity Characterization at Landscape Level (BCLL) initiated by Indian space research institute (ISRO, Dehradun). The large database is available for free access at (http://bis.iirs.gov.in/). The nested quadrat represents 20 × 20 m² for the tree (> 15 cm cbh) and lianas, two 5 × 5 m² plots for shrubs and sapling (> 5 to < 10 cm cbh), four 1 m² plots for herbs and seeding were recorded in designated forms with appropriate species identification and site characteristics [43]. The geo-tagged plant database optimized sampling sufficiency at vegetation type's level using stratified random sampling. The quadrat-wise species richness (count of unique species in a plot) data was pooled from the national database for the Western Ghats region. There are 891 sample points laid over the forest area are considered for analysis (Fig. 1). The number of species (species richness) with respect to each quadrat location was utilized in the analysis (Fig. 1b, Table 1).

Fig. 1 a Forest cover map of the Western Ghats, derived from the Vegetation type map of India [38]; b Map showing the distribution of 891 field sampling quadrats distribution in the study area (as per [43]); the species richness (i.e., number of species) varies from 1 to 48 per quadrat
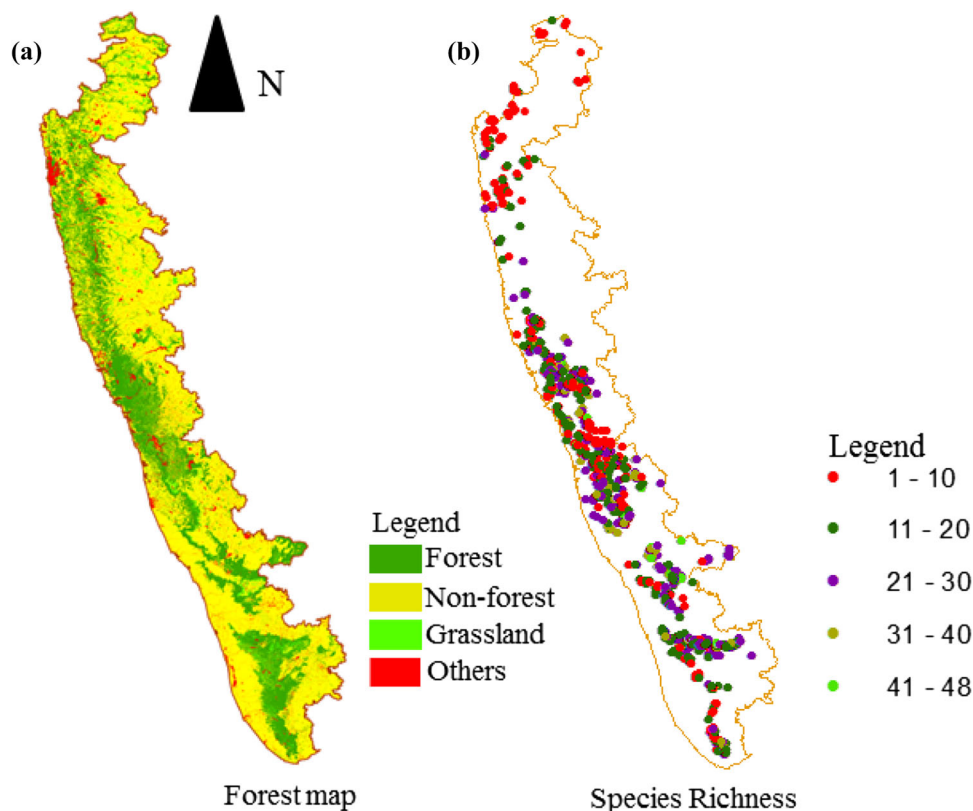

Table 1 The frequency distribution of 891 field sampling quadrats in the study area (as per [43])

Species richness	Quadrat	Species richness	Quadrat	Species richness	Quadrat
1	3	17	51	33	18
2	2	18	40	34	8
3	4	19	49	35	7
4	7	20	43	36	4
5	11	21	42	37	3
6	7	22	40	38	1
7	1	23	40	39	1
8	17	24	35	40	5
9	21	25	28	41	2
10	19	26	39	42	1
11	29	27	30	43	2
12	31	28	25	44	1
13	18	29	17	45	1
14	42	30	16	46	1
15	48	31	14	47	2
16	42	32	13	48	1

2.3 MODIS Vegetation Indices

Moderate Resolution Imaging Spectroradiometer (MODIS) data products are available since 2000 at various spatial resolutions (i.e., 250 m, 500 m, 1000 m) at daily to monthly interval. For this study, the data were downloaded for the year of 2000. The MODIS derived vegetation indices, band composition, and peculiarities are important to explain the vegetation pattern [44]. The spatial

resolution of 500 m data was downloaded for SR-645nm (MOD09A1), SR-858nm (MOD09A1), *f*PAR (MOD15A2H), LAI (MOD15A2H), EVI (MOD13A1) and NDVI (MOD13A1) (https://modis.gsfc.nasa.gov/, https://reverb.echo.nasa.gov/).

2.3.1 Spectral Absorbance Properties

The MODIS surface reflectance product derived by using 6 s radiative transfer model that considered performed using aerosols (MOD04), water vapor (MOD05), ozone (MOD07) and cloud mask (MOD35) for atmospheric correction. The MODIS derived surface reflectance SR-645nm (MOD09A1) and SR-858nm (MOD09A1) is the 8-days interval data available at 500 m spatial resolution in the range of 620–670 nm, and 841–876 nm respectively.

2.3.2 Based on Biomass Storage

The two vegetation indices i.e., NDVI and EVI were derived using MODIS surface reflectance product from the band blue (459–479 nm), red (600–680 nm) and near-infrared (846–885 nm) region [45]. NDVI is simple and widely used vegetation index using NIR and red band:

$$NDVI = \frac{(NIR - R)}{(NIR + R)}$$

The MODIS derived EVI algorithm also includes the blue band to minimize the aerosol influence by the red bands:

$$EVI = \frac{(NIR - R)}{(NIR + C1 \times R - C2 \times B + L)}$$

The adopted coefficients are, Canopy background adjustment (L) = 1, Coefficients of the aerosol resistance term: C1 = 6, C2 = 7.5, G (gain factor) = 2.5

2.3.3 Based on Canopy Density and Structure

MODIS algorithm to derive LAI and *f*PAR considered atmospherically corrected BRDF, a three-dimensional (3–D) radiative transfer model (derive spectral and angular biome-specific signatures of vegetation canopies) and MODIS land cover product (MOD12) [46, 47].

All data were projected using MODIS re-projection tool (MRT). Further, processing that includes scaling, normalization and masking for the study area is performed using ArcGIS [48, 49]. Final data compilation was carried out at the temporal resolution of monthly average, seasonal and annual. The 16-days data intervals were averaged to generate monthly and subsequently annual data. The 4 months data from June to September was analyzed for monsoon to capture the maximum plant growth that may have better

reflectance and species richness patterns. There are 891 sampling plots recorded from the forest area of Western Ghats. For each plot species richness was assessed and compiled to point shape file where each plot denoted with a unique id as point. Using ArcGIS the reflectance values for each ground sampled point (total 891 plot each marked a one point) of forest area were extracted for all the six MODIS vegetation proxies. Further, sampling plot having more than 50% tree species defined as woody plot while non-woody plots identified those were dominated by more shrubs or herbs. Similarly, the woody and non-woody plots species richness variation with annual and monsoon period was analyzed for *f*PAR and LAI.

2.4 Statistical Analysis

The species richness with respect to each MODIS derived vegetation indices regressed linearly. The model evaluation and output interpretation is based on R^2 value and slope (Table 2). The statistical distribution concerning vegetation surrogate derived from MODIS observed to have a better fitting with linear and descriptive than smooth fitting. Hence the interpretations are based on linear fitting output. However, the two curves resemble each other unless very few sampled at targeted data range. Graphically, the fitted modelled for species richness with individual vegetation index was performed using R software (CRAN ggplot).

3 Results and Discussion

3.1 Species Richness Relation with MODIS Vegetation Indices

Using 891 randomly sampled nested quadrat plots in forest area and its relation with MODIS derived vegetation indices was analyzed for the Western Ghats. The comprehensive ground sampled data is randomly distributed, and no clustering effect of skewness was observed. Plot wise species richness were assessed and observed to be varied from minimum 1 to maximum 48 (Fig. 1b). The majority of the plot (51) out of 891 is having species richness of 17 (Table 1). The plot density as well as the range of vegetation indices also varies from medium to higher range for all the six MODIS vegetation indices that infer study sites have diverse and dense forest canopy (Figs. 3, 4, 5, 6, 7). The species co-existence addressed the diversity and distribution, which enhance productivity by symbiotically access, share and recycled nutrient resources to grow together [4–6]. Both spatially or ground measured of productivity can be performed through chlorophyll concentration and reflectance, leaf area, light absorbance or reflectance by species. The ground variability of species

Table 2 Showing the linear fitting of each vegetation indices (annual, monsoon) with species richness, (Refer: ns=non-significant, nw=non-woody, w-woody)

MODIS index	Annual		Post-monsoon	
	R^2	Slope	R^2	Slope
SR-645nm	0.05	− 59.4	0.006	− 15.4
SR-858nm	0.003	− 18.6	ns	− 4.6
NDVI	0.07	23.9	0.02	17
EVI	0.04	31.2	0.006	11.4
fPAR	0.05	14.5	0.01	10.4
	w-0.08, nw-ns	w-17.7, nw-(−0.4)	w-0.01, nw-ns	w-11.6, nw-5.5
LAI	0.03	1.1	0.02	1.2
	w-0.07, nw-ns	w-1.6, nw-(0.69)	w-0.04, nw-ns	w-1.6, nw-(−0.6)
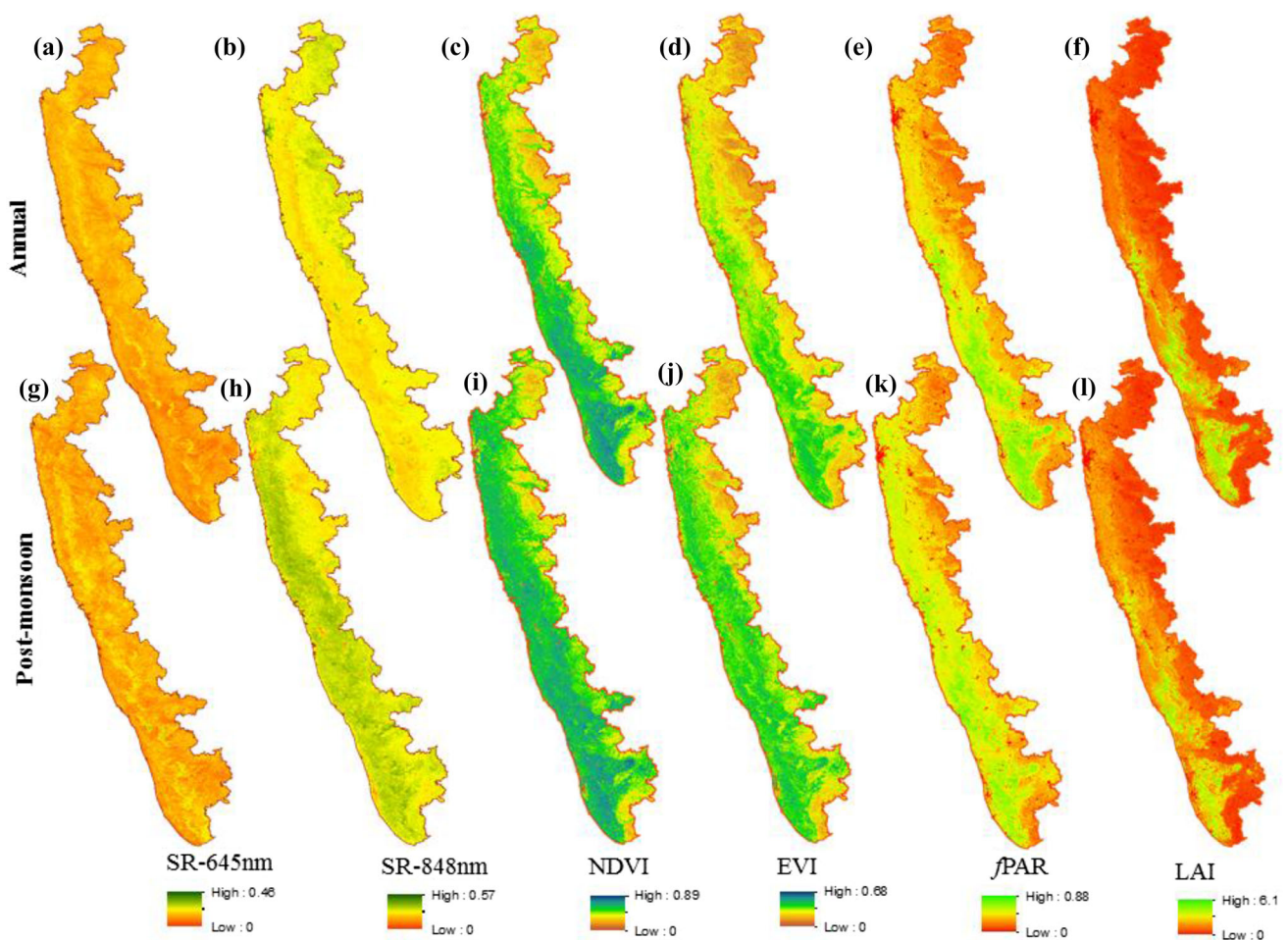
Fig. 2 The images showing 2-reflectance bands (at 645 and 848 nm) and 4-biophysical variables (i.e., NDVI, EVI, fPAR and LAI) derived from MODIS instruments during annual and post-monsoon period

represents the spatial heterogeneous canopy cover, which captured the spectral heterogeneity from the remote sensor [7]. For monoculture or managed forests have good spectral signature hence the accuracy to predict species richness using biophysical proxies is nearly 70%. NDVI explained 61% of tree species richness tested for 59 homogeneous ground sampled plot in Western Ghats [32]. Here, we used 891 random plots in the total forest area of the Western Ghats for 2-reflectance bands (at 645 and 848 nm) and 4-biophysical variables (i.e., NDVI, EVI, fPAR and LAI)
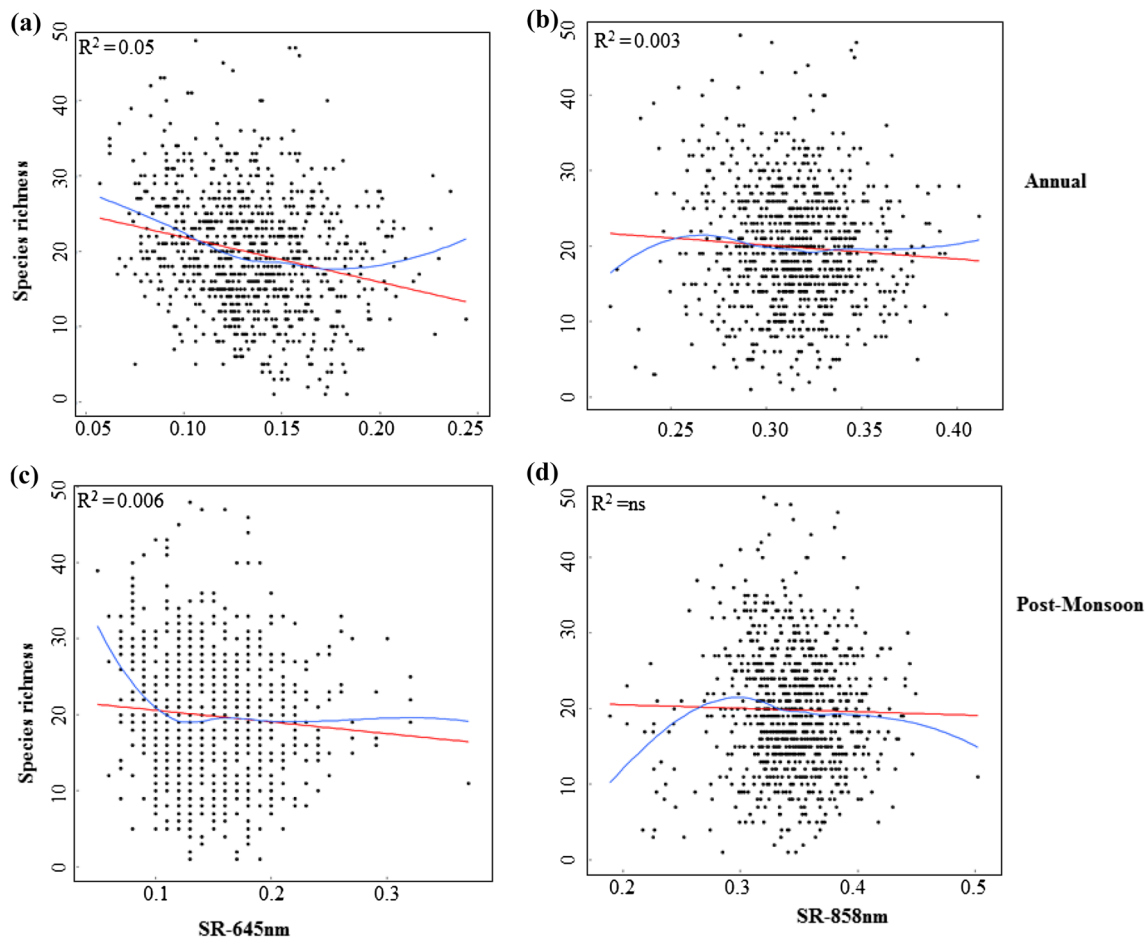
Fig. 3 Scatter plots for SR-645nm and SR-858nm shown against species richness, where (**a**, **b**) for annual and (**c-d**) for post-monsoon period, (where ns refers to non-significant)

derived from MODIS instruments during annual and post-monsoon period.

3.2 Surface Reflectance (SR-645nm and SR-858nm)

The range of surface reflectance for SR-645nm is from 0 to 0.45, while 0 to 0.57 for SR-858nm (Fig. 2a, b, g, h). The relationship between species richness to SR-645nm have negative slope fitting with poor R^2 value (0.05). As per SR-645nm, majority of species richness points are distributed in between 0.11 to 0.14 (Fig. 3a). Similarly, the range for SR-858nm from 0.28 to 0.37 (Fig. 3b). The highest species richness distribution was between 0.1 to 0.14 for SR-645nm, and 0.28 to 0.30 for SR-858 nm. The model fitting resulted better for SR-645 nm with species richness compared to SR-858 nm. From annual to monsoon, the range vegetation indices with respect to sample plots distribution seems to be enhanced for SR-645nm from 0.25 to 0.4 (Fig. 3c, d). Similarly, for SR-645nm the annual range was 0.45, which made up to 0.55 in monsoon (Fig. 3c, d). The absorption spectra where finished its species distribution

the reflectance spectra resumed from that point, which is clearly interpreted for both annual or monsoon period (Fig. 3). The slope for both SR-645nm and SR-858nm observed to have negative for species richness (Table 2).

Among the two MODIS derived surface reflectance bands, one is red absorbance (SR-645nm) and another infra-red reflectance (SR-858nm) region of the photosynthetically active radiation (Fig. 2a, b). Monsoon invites germination of new species and enhance photosynthesis of both new and existing using light energy. Therefore, the range of SR-645nm is comparatively more due to more light absorption in monsoon for photosynthesis than annual (Fig. 3a, c). Similarly, with the increase in photosynthesis, productivity and species reflectance also increases. Hence more reflectance from new leaves or canopy surface have enhanced reflectance for monsoon than annual SR-858nm (Fig. 3b, d). More diversity leads to more species richness that resembles positively to surface reflectance that could better explain the relationship and helpful to mapped the generous species distribution the complexity in heterogeneous environments [14]. Overall, we observed positive
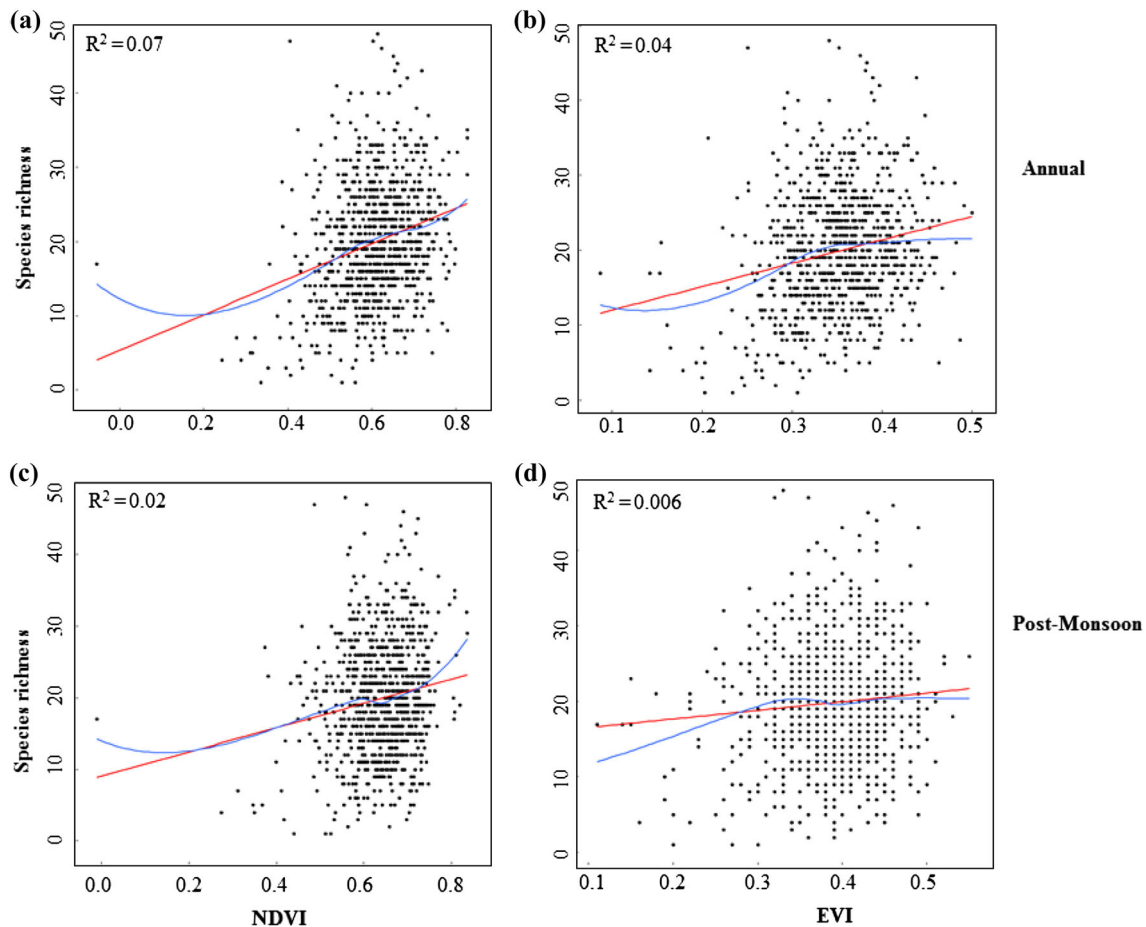
Fig. 4 Scatter plots for NDVI and EVI shown against species richness, where (**a**, **b**) for annual and (**c**, **d**) for post-monsoon period

pattern for species richness and surface reflectance for annual and monsoon (except SR-848nm, monsoon).

3.3 NDVI and EVI

The pattern of richness is distinguished and positively ranging up to 0.89 for NDVI and 0.68 for EVI (Fig. 2c, d, i, j). The species having the range less than 0.2 NDVI and 0.1 EVI perhaps not distributed in forest area of the Western Ghats (one exception out of 891 quadrats). The majority of sampled data distributed in the range of 0.4–0.8 NDVI and the highest species richness covered in between 0.6 to 0.7 NDVI (Fig. 4a). In other hand, the distributions of maximum sample points are in between 0.3 to 0.5 EVI. The highest species richness recorded in between 0.35 to 0.39 for EVI (Fig. 4b). The monsoon versus annual NDVI and EVI derived a clearer pattern with respect to species richness. Few distribution of species ranged towards the highest range of NDVI (0.8) in monsoon than annual (Fig. 4a, c). Similarly, the range of EVI enhanced from 0.5 annual to 0.6 for the monsoon period (Fig. 4b, d).

The relationship observed to be positive for both NDVI and EVI with species richness where the range of distribution has expanded for monsoon season (Fig. 4). As during monsoon season, more new leaf formation contains fresh chlorophyll pigments. Both NDVI and EVI are sensitive to pigment concentration, which optimized the monsoon response compared to annual average. Comparing with NDVI the range of EVI is less, as NDVI has limitation to saturate in dense forest; the Western Ghats being a hotspot of biodiversity holds diverse and dense forest all along. The analysis of species richness with NDVI in addition to other productivity indices minimizes the strength of NDVI to explain richness [21]. However, in particular NDVI with species richness have derived positive relation to explain the pattern better. Sometimes, NDVI has emerged as a comparatively better proxy for species richness of Western Ghats [19]. Oppositely, NDVI observed as a weakly correlating variable to explain species richness [17].
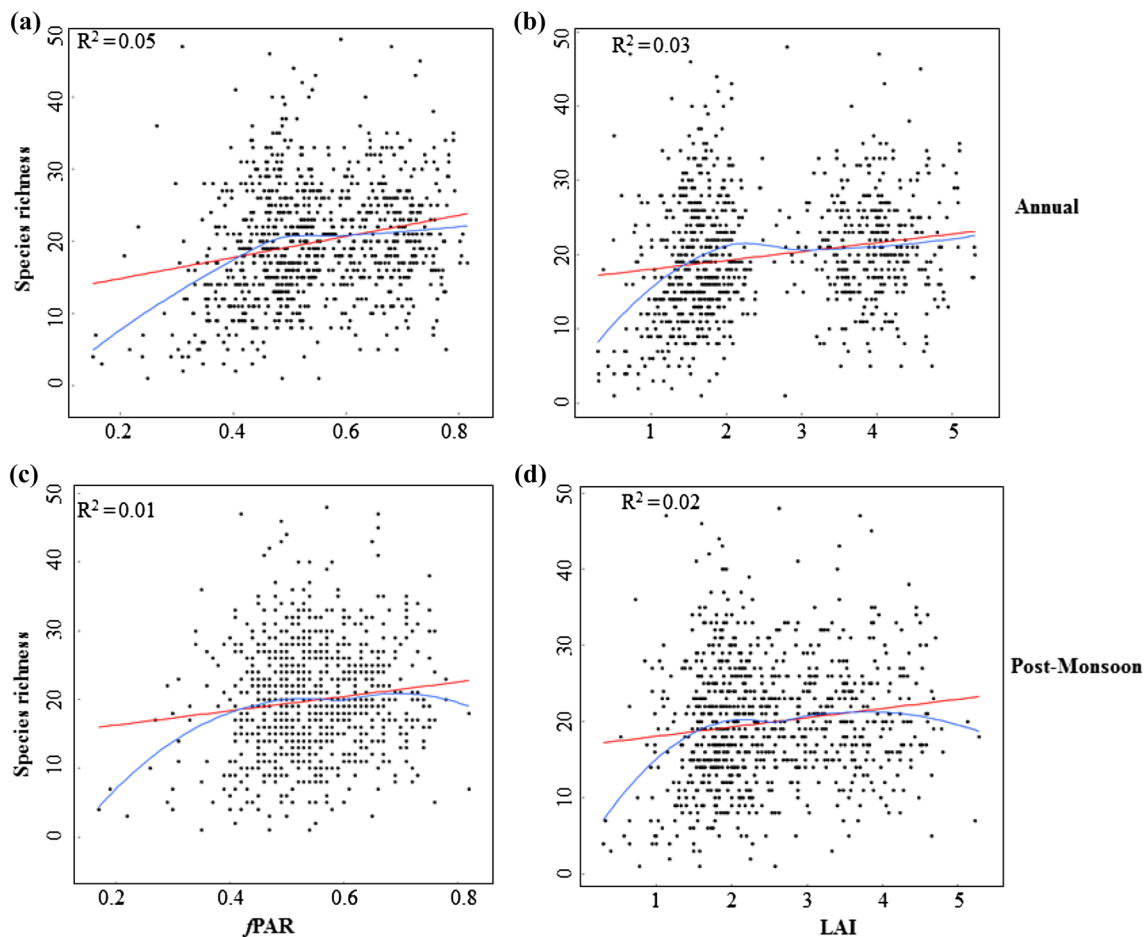
Fig. 5 Scatter plots for fPAR and LAI shown against species richness, where (**a**, **b**) for annual and (**c**, **d**) for post-monsoon period

3.4 *f*PAR and LAI

The *f*PAR range varies from 0 to 0.88, while LAI is from 0 to 6.1 (Fig. 2e, f, k, l). The species richness for *f*PAR varies between 0.4 and 0.8, which holds the majority of sample strength. The highest species richness corresponds to *f*PAR ranges are distributed near 0.5 and 0.7 (Fig. 5a). The major distribution of sample observed between 1 to 2 LAI and again from 0.35 to 4.8 ranges. The maximum species richness also holds in both ranges of LAI. A range gap observed from 2.5 to 3 LAI ranges where limited number species are distributed. Perhaps, the species falling under that range of LAI distribution are abundant in the Western Ghats (Fig. 5b). The monsoon pattern of *f*PAR and LAI considerably different than annual. The *f*PAR and LAI range for annual and monsoon remain same, but the uniformity in distribution marked in monsoon (Fig. 5c). Another hand, the gap observed between 2.5 to 3 for LAI in annual became generously filled with monsoon plant species (Fig. 5d).

The statistically fitting of species richness is positive for both *f*PAR and LAI (Fig. 5). The *f*PAR with respect to species richness have the uniform pattern. The wide range of *f*PAR interprets the availability of open forest to more dense, that are photosynthetically more active and productive forest in the Western Ghats. Also, LAI range is high and could reach up to 6.1 in Western Ghats; whereas researchers of the great Amazon rainforest have the LAI range of 6–7 [25]. The range of LAI explains the distribution of grassland or herbs to the tall and large canopy based plant distribution in the Western Ghats. Therefore, the Western Ghats is considered as an important region to have wide range of plant diversity and distribution. The annual distribution of LAI expected to have two groups i.e., non-woody towards the lower LAI range, while woody species occupy the higher extent (Fig. 5). The monsoon LAI distribution of species richness also holds sample point for the range 2.5–3 of LAI. This reported the distribution of seasonal species also holds a distinct range of distribution with respect to vegetation indices that remain suppressed in annual variability.
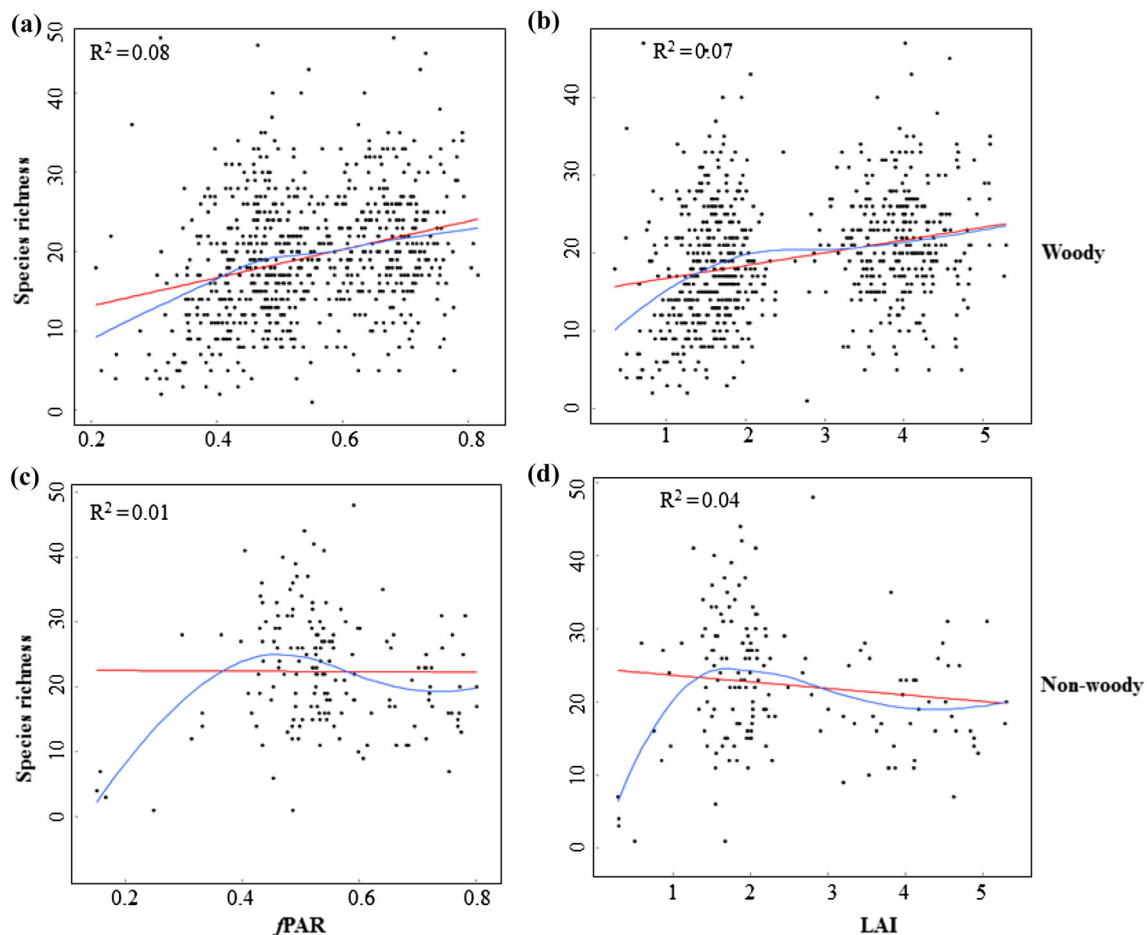
Fig. 6 Scatter plots showing distribution of annual fPAR and annual LAI, with woody species (**a**, **b**) and non-woody species (**c**, **d**)

3.5 Woody/Non-woody (fPAR and LAI)

3.5.1 Annual

The sample plots having more than 50% tree species were considered as woody plot and the remaining as non-woody. There are 726 plots recorded under woody categories and 165 as non-woody plots. The distribution of woody species pattern concerning fPAR and LAI resembles with the overall pattern shown in Fig. 5. Additionally, the statistical fitting (R^2 value) increases from 0.05 to 0.08 for the fPAR woody, and 0.03 to 0.07 in case of woody species richness plot compare to the whole (Table 2). The ranges of distribution for the woody or non-woody species remain unchanged for both fPAR and LAI (Fig. 6). However, the majority of species ranges between 0.4 to 0.6 for fPAR while 1.5 to 3 for LAI (Fig. 6c, d). The statistics of fitting woody species with fPAR ($R^2 = 0.08$) and LAI ($R^2 = 0.07$) are positive, while very weak for non-woody ($R^2 = 0.01$) for fPAR and ($R^2 = 0.07$) LAI (Fig. 6). The negative relation of non-woody may infer less simple leaf architecture with less density.

Our objective was to identify the distribution of woody and non-woody species as per fPAR and LAI range could provide insights to ecology of the Western Ghats. The woody species occupy the majority of species along the wide range of vegetation indices. The range of maximum LAI reported up to 3 from Ruokolahti coniferous forest and proved to have positive fitting of LAI with woody species [30]. However, non-woody species occupy the medium range in fPAR while low LAI range. It describes that the low canopy cover (non-woody) species are mostly seasonal, hence could made their contribution up to the lower LAI range. A linear pattern between field measured tree species richness of broadleaf forest with MODIS fPAR and LAI was reported in Petersham, United States [28].

3.5.2 Monsoon

The monsoon period best explain the plant life-cycle. Mostly, the non-woody can be figured in monsoon as their life-span is short and maximum growth achieved in during this period. The maximum woody species is ranged between 0.4 and 0.8 for fPAR (Fig. 7a). Similarly, LAI
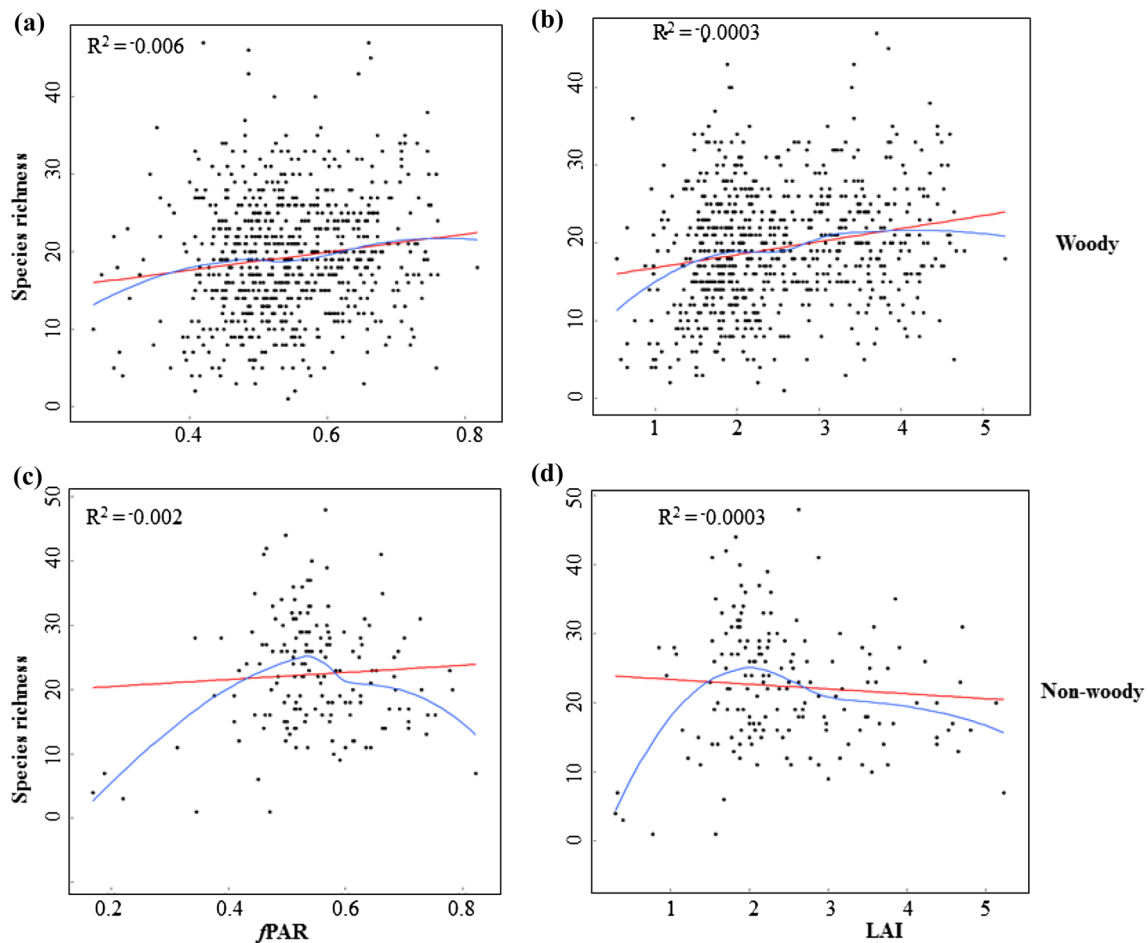
Fig. 7 Scatter plots showing distribution of post-monsoon period *f*PAR and LAI, with woody species (**a**, **b**) and non-woody species (**c**, **d**), (where ns refers to non-significant)

ranged between 1 to 2.5 for maximum woody species richness. The distribution of non-woody species observed between 0.5 to 0.6 for *f*PAR, while 1.5 to 2.5 maximum species richness for LAI observed. Also, along with non-woody species the woody species are present in the range of 2–3 (Fig. 7b, d).

The variability of woody and non-woody distribution for *f*PAR and LAI was assumed to capture the seasonal species distribution. Here, the distribution for *f*PAR is nearly same with annual pattern of woody and non-woody species. However, the LAI range holds a complete range of woody species distributed from 1 to 5.3 (Fig. 7b). In addition to woody species, the seasonal non-woody species also distributed between the range of 2.5–3; which remain suppressed in annual LAI pattern with species richness (Figs. 5b, 7d). The non-woody holds the open canopy architecture that more clearly define the species for LAI pattern variation. As observed for boreal forest the incorporation of non-woody vegetation into the validation enhanced the ground observed to MODIS derived

correlation compared only to woody species distribution in northern Canada [50].

The overall positive relationship was observed in four vegetation proxies (NDVI, EVI, LAI and *f*PAR), while negative pattern fitting observed for SR-645nm and SR-858nm (Fig. 3). Statistically, each MODIS vegetation indices fitted with positive R^2 values although weakly related, except SR-858nm (monsoon). The model fitting was relatively good for annual NDVI (0.07) for total species richness of 891 plots in Western Ghats (Table 2). The probable reason for weak positive pattern could be the more moisture availability in the atmosphere as Western Ghats is moist region; secondly the mixed pixel also affects the relationship to become weaker [10, 18]. The analysis of woody species versus non-woody species summarized the robust model fitting with R^2 0.08 for *f*PAR with woody species. The non-woody species with annual or monsoon distribution have non-significant R^2 for both *f*PAR and LAI (Table 2).

4 Conclusions

In general, annual pattern of correlation faired than seasonal (i.e., monsoon) between biophysical variables and species richness. The woody subset of the species demonstrated better relation with the biophysical variables at annual scale. Although, each index explains the distribution pattern differently, the model fitting of NDVI with species richness is comparatively better. NDVI ranges relatively high due to its sensitivity to photosynthetic pigments. However, the same species richness and distribution, EVI range is relatively lower than NDVI. This is due to their differences in algorithm, utilized for correction fact or in the blue band. The distribution of fPAR found very high (0.4–0.8) and the species of different absorbance range are distributed in the study site. The annual LAI derived two distinct clusters that minimize the effect of seasonal species distribution. The monsoon species richness pattern shows LAI clearly represents the seasonality in the Western Ghats. The relation between the species richness to biophysical proxies are positive. They show poor correlation, but the expandability varies from medium to high. The correlation is likely to improve by considering homogeneous pixel for forest area or by down scaling to high resolution satellite imagery.

References

1. Levin N, Shmida A, Levanoni O, Tamari H, Kark S (2007) Predicting mountain plant richness and rarity from space using satellite-derived vegetation indices. Divers Distrib 13:692–703
2. Phillips LB, Hansen AJ, Flather CH, Robison-Cox J (2010) Applying species–energy theory to conservation: a case study for North American birds. Ecol Appl 20:2007–2023
3. Tucker CJ, Pinzon JE, Brown ME, Slayback DA, Pak EW, Mahoney R, Vermote EF, El Saleous N (2005) An extended AVHRR 8-km NDVI dataset compatible with MODIS and SPOT vegetation NDVI data. Int J Remote Sens 26:4485–4498
4. Diamond J (1988) Factors controlling species diversity: overview and synthesis. Ann Mo Bot Gard 75:117–129
5. Carlson KM, Asner GP, Hughes RF, Ostertag R, Martin RE (2007) Hyperspectral remote sensing of canopy biodiversity in Hawaiian lowland rainforests. Ecosystems 10:536–549
6. Colwell RK, Coddington JA (1994) Estimating terrestrial biodiversity through extrapolation. Philos Trans R Soc B 345:101–118
7. Nagendra H (2001) Using remote sensing to assess biodiversity. Int J Remote Sens 22:2377–2400
8. Rey-Benayas JM, Pope KO (1995) Landscape ecology and diversity patterns in the seasonal tropics from Landsat TM imagery. Ecol Appl 5:386–394
9. Gould W (2000) Remote sensing of vegetation, plant species richness, and regional biodiversity hotspots. Ecol Appl 10:1861–1870
10. Rocchini D (2007) Effects of spatial and spectral resolution in estimating ecosystem alpha-diversity by satellite imagery. Remote Sens Environ 3:423–434
11. Lauver C (1997) Mapping species diversity patterns in the Kansas shortgrass region by integrating remote sensing and vegetation analysis. J Veg Sci 8:387–394
12. Gessner U, Machwitz M, Conrad C, Dech S (2013) Estimating the fractional cover of growth forms and bare surface in savannas. A multi-resolution approach based on regression tree ensembles. Remote Sens Environ 129:90–102
13. Viña A, Tuanmu MN, Xu W, Li Y, Qi J, Ouyang Z, Liu J (2012) Relationship between floristic similarity and vegetated land surface phenology: implications for the synoptic monitoring of species diversity at broad geographic regions. Remote Sens Environ 121:488–496
14. Morán-Ordóñez A, Suárez-Seoane S, Elith J, Calvo L, de Luis E (2012) Satellite surface reflectance improves habitat distribution mapping: a case study on heath and shrub formations in the Cantabrian Mountains (NW Spain). Divers Distrib 18:588–602
15. Puzachenko YG, Sandlersky RB, Sankovski AG (2016) Analysis of spatial and temporal organization of biosphere using solar reflectance data from MODIS satellite. Ecol Model 341:27–36
16. Jackson TJ, Daoyi C, Michael C, Fuqin L, Martha A, Charles W, Paul D, Hunt ER (2004) Vegetation water content mapping using Landsat data derived normalized difference water index for corn and soybeans. Remote Sens Environ 92:475–482
17. Rocchini D, Chiarucci A, Loiselle SA (2004) Testing the spectral variation hypothesis by using satellite multispectral images. Acta Oecol 26:117–120
18. Ozkan UY, Ozdemir I, Saglam S, Yesil A, Demirel T (2016) Evaluating the woody species diversity by means of remotely sensed spectral and texture measures in the urban forests. J Indian Soc Remote Sens 44:687–697
19. Bawa K, Rose J, Ganeshaiah KN, Barve N, Kiran MC, Umashanker R (2002) Assessing biodiversity from space: example from Western Ghats, India. Conserv Ecol 6:1–7
20. Seto KC, Fleishman E, Fay JP, Betrus CJ (2004) Linking spatial patterns of bird and butterfly species richness with Landsat TM derived NDVI. Int J Remote Sens 25:4309–4324
21. Phillips LB, Andrew JH, Curtis HF (2008) Evaluating the species energy relationship with the newest measures of ecosystem energy: NDVI versus MODIS primary production. Remote Sens Environ 112:4381–4392
22. John R, Jiquan C, Nan L, Ke G, Cunzhu L, Yafen W, Asko N, Keping M, Xingguo H (2008) Predicting plant diversity based on remote sensing products in the semi-arid region of Inner Mongolia. Remote Sens Environ 112:2018–2032
23. Huete A, Didan K, Miura T, Rodriguez EP, Gao X, Ferreira LG (2002) Overview of the radiometric and biophysical performance of the MODIS vegetation indices. Remote Sens Environ 83:195–213
24. Peng D, Chaoyang W, Cunjun L, Xiaoyang Z, Zhengjia L, Huichun Y, Shezhou L, Xinjie L, Yong H, Bin F (2017) Spring green-up phenology products derived from MODIS NDVI and EVI: intercomparison, interpretation and validation using National Phenology Network and AmeriFlux observations. Ecol Ind 77:323–336
25. Hilker T, Lyapustin AI, Hall FG, Myneni R, Knyazikhin Y, Wang Y, Tucker CJ, Sellers PJ (2015) On the measurability of change in Amazon vegetation from MODIS. Remote Sens Environ 166:233–242
26. Lafage D, Jean S, Anita G, Jan-Bernard B, Julien P (2014) Satellite-derived vegetation indices as surrogate of species richness and abundance of ground beetles in temperate floodplains. Insect Conserv Divers 7:327–333
27. Waring RH, Coops NC, Fan W, Nightingale JM (2006) MODIS enhanced vegetation index predicts tree species richness across forested ecoregions in the contiguous USA. Remote Sens Environ 103:218–226

28. Shabanov NV, Wang Y, Buermann W, Dong J, Hoffman S, Smith GR, Tian Y, Knyazikhin Y, Myneni RB (2003) Effect of foliage spatial heterogeneity in the MODIS LAI and FPAR algorithm over broadleaf forests. Remote Sens Environ 85:410–423

29. Saatchi S, Buermann W, TerSteege H, Mori S, Smith TB (2008) Modeling distribution of Amazonian tree species and diversity using remote sensing measurements. Remote Sens Environ 112:2000–2017

30. Wang Y, Woodcock CE, Buermann W, Stenberg P, Voipio P, Smolander H, Häme T, Tian Y, Hu J, Knyazikhin Y, Myneni RB (2004) Evaluation of the MODIS LAI algorithm at a coniferous forest site in Finland. Remote Sens Environ 91:114–127

31. Nagendra H, Gadgil M (1999) Satellite imagery as a tool for monitoring species diversity: an assessment. J Appl Ecol 36:388–397

32. Singh TP, Das S (2014) Predictive analysis for vegetation bio-mass assessment in Western Ghat region (WG) using geospatial techniques. J. Indian Soc. Remote Sens. 42:549–557

33. Nagendra H, Ghate U (2003) Landscape ecological planning through a multi-scale characterization of pattern: studies in the Western Ghats, South India. Environ Monit Assess 87:215–233

34. Kumar A, Uniyal SK, Lal B (2007) Stratification of forest density and its validation by NDVI analysis in a part of western Himalaya, India using Remote sensing and GIS techniques. Int J Remote Sens 28:2485–2495

35. Pau S, Thomas WG, Elizabeth MW (2012) Dissecting NDVI–species richness relationships in Hawaiian dry forests. J Biogeogr 39:1678–1686

36. Tonkin JD, Bogan MT, Bonada N, Rios-Touma B, Lytle DA (2017) Seasonality and predictability shape temporal species diversity. Ecology 98:1201–1216

37. Bender I, Kissling WD, Böhning-Gaese K, Hensen I, Kühn I, Wiegand T, Dehling DM, Schleuning M (2017) Functionally specialised birds respond flexibly to seasonal changes in fruit availability. J Anim Ecol 86:800–811

38. Roy PS, Behera MD, Murthy MS, Roy A, Singh S, Kushwaha SP, Jha CS, Sudhakar S, Joshi PK, Reddy CS, Gupta S et al (2015) New vegetation type map of India prepared using satellite remote sensing: comparison with global vegetation maps and utilities. Int J Appl Earth Obs Geoinf 39:142–159

39. Gunawardene NR, Daniels DA, Gunatilleke IA, Gunatilleke CV, Karunakaran PV, Nayak GK, Prasad S, Puyravaud P, Ramesh BR, Subramanian KA, Vasanthy G (2007) A brief overview of the Western Ghats-Sri Lanka biodiversity hotspot. Curr Sci 93:1567–1572

40. Pascal JP, Ramesh BR, DE Franceschi D (2004) Wet evergreen forest types of the south Western Ghats, India. Trop Ecol 45(2):281–292

41. Ramesh BR, Menon S, Bawa KA (1997) vegetation-based approach to biodiversity gap analysis in Agasthyamalai region, Western Ghats, India. Ambio 28:529–536

42. Chitale VS, Behera MD, Roy PS (2014) Future of endemic flora of biodiversity hotspots in India. PLoS ONE 9:1–15

43. Roy PS, Kushwaha SPS, Murthy MSR, Roy A, Kushwaha D, Reddy CS, Behera MD, Mathur VB, Padalia H, Saran S, Singh S, Jha CS, Porwal MC (2012) Biodiversity Characterisation at landscape level: national assessment. Indian Institute of Remote Sensing, Dehradun, p 140. ISBN 81-901418-8-0

44. Hobi ML, Dubinin M, Graham CH, Coops NC, Clayton MK, Pidgeon AM, Radeloff VC (2017) A comparison of Dynamic Habitat Indices derived from different MODIS products as predictors of avian species richness. Remote Sens Environ 195:142–152

45. Wardlow BD, Stephen LE (2010) A comparison of MODIS 250-m EVI and NDVI data for crop mapping: a case study for southwest Kansas. Int J Remote Sens 31:805–830

46. Knyazikhin Y, Martonchik JV, Myneni RB, Diner DJ, Running SW (1998) Synergistic algorithm for estimating vegetation canopy leaf area index and fraction of absorbed photosynthetically active radiation from MODIS and MISR data. J Geophys Res 103:32257–32277

47. Tian Y, Zhang Y, Knyazikhin Y, Myneni RB, Glassy JM, Dedieu G, Running SW (2000) Prototyping of MODIS LAI and FPAR algorithm with LASUR and LANDSAT data. IEEE Trans Geosci Remote Sens 38:2387–2401

48. ESRI, ESRI, Redlands CA (2004) ArcGIS, New York

49. Tim Ormsby (2004) Getting to know ArcGIS desktop: basics of ArcView, ArcEditor, and ArcInfo. ESRI Inc., Redlands

50. Serbin SP, Douglas EA, Stith TG (2013) Spatial and temporal validation of the MODIS LAI and FPAR products across a boreal forest wildfire chronosequence. Remote Sens Environ 133:71–84